

SCALING THE FEEDING MECHANISM OF LARGEMOUTH BASS (*MICROPTERUS SALMOIDES*): KINEMATICS OF PREY CAPTURE

BARTON A. RICHARD AND PETER C. WAINWRIGHT*

Department of Biological Science, Florida State University, Tallahassee, FL 32306-3050, USA

Accepted 15 September 1994

Summary

We present the first analysis of scaling effects on prey capture kinematics of a feeding vertebrate. The scaling of feeding kinematics of largemouth bass (*Micropterus salmoides*) was investigated using high-speed video (200 fields s⁻¹) to determine what functional changes occur in the feeding mechanism as a consequence of body size. A size series of ten bass ranging from 32 to 210 mm standard length was used for the study and ten feeding sequences from each individual were analyzed to quantify movements of the feeding apparatus during prey capture. Maximal linear and angular displacements of the strike scaled isometrically. The time course of the strike was longer in larger fish. Maximal velocities of displacement were more rapid in larger fish, but their scaling exponents indicated that the intrinsic rate of muscle shortening decreased with fish size. Morphological measurements of the lever arms of the lower jaw and of the two major muscles that drive the

feeding mechanism were made to relate possible biomechanical changes in the feeding mechanism to the observed kinematic relationships. The lever arms of the lower jaw and the muscles scaled isometrically; hence, the relative slowing of movements with increasing body size cannot be attributed to changes in mechanical advantage with change in body size. The scaling of feeding kinematics in the largemouth bass is in accord with the scaling of rates of muscle contraction found in other lower vertebrates. These findings demonstrate that body size can have major effects on feeding kinematics and that future comparative studies of feeding kinematics should use empirical data on size effects in kinematic comparisons between taxa.

Key words: scaling, kinematics, prey capture, largemouth bass, *Micropterus salmoides*, feeding, behaviour.

Introduction

Body size is one of the most important attributes of an organism from both an ecological and evolutionary standpoint. Size can enable or constrain an animal's abilities to function in and exploit its environment. Scaling studies deal with the structural and functional consequences of change in size (Calder, 1984; Schmidt-Nielsen, 1984). Kinematic studies are often used to quantify the performance of various animal functions. Kinematic analyses involve discerning patterns of displacement of one or more components of a mechanism and, usually, calculating the various variables of displacement, such as velocities, accelerations and the timing of movements. The effect of body size on kinematic output has been the subject of considerable study in the locomotion literature (Garland, 1985; Marsh, 1988; Bennett *et al.* 1989; Katz and Gosline, 1993), but has thus far been overlooked in the feeding literature. Yet, it is likely that changes in the functional ability of feeding mechanisms will occur with changes in body size both within and among taxa.

The kinematics of prey capture have been the subject of extensive study in numerous vertebrate taxa, including fishes

(Alexander, 1969; Nyberg, 1971; Liem, 1978; Lauder, 1983, 1985; Westneat, 1990), salamanders (Shaffer and Lauder, 1988; Larsen and Beneski, 1988; Reilly and Lauder, 1992; Schwenk and Wake, 1993), frogs (Gans and Gorniak, 1982; Nishikawa and Cannatella, 1991), squamate reptiles (Schwenk and Throckmorton, 1989; Smith, 1982, 1984), birds (Zweers, 1974) and mammals (Hiimae *et al.* 1981; Hiimae and Crompton, 1985; Thexton and Crompton, 1989). The above citations represent only a sample of the many papers that quantify the kinematic patterns of prey capture in numerous species. Investigators have often, but not always, attempted to limit the size range of experimental animals in the hope of controlling for variation within and among species caused by body size, but have rarely directly considered the subject of body size. Comparative studies between species using kinematic data have been carried out (Shaffer and Lauder, 1985; Larsen *et al.* 1989; Miller and Larsen, 1990; Reilly and Lauder, 1992) and will probably become much more common in the future.

In order to investigate the potential for size-induced effects

*Author for correspondence.

on prey capture kinematics, we completed a study of the scaling of feeding kinematics of largemouth bass (*Micropterus salmoides*). The goal was to determine what functional changes occur in the feeding mechanism with increase in body size. Two mechanical models were used to generate expected changes in feeding kinematics, assuming the maintenance of geometric similarity and functional equivalence with increasing size. The observed scaling of kinematic output was then compared with that given by the models.

Materials and methods

The largemouth bass (*Micropterus salmoides*) was chosen for this study because its large feeding apparatus is well suited to the goal of quantifying patterns of movement of the musculo-skeletal elements of the feeding mechanism. *Micropterus salmoides*, the largest member of the family Centrarchidae, typically reaches sexual maturity at about 200mm standard length (SL) and can reach up to 900mm in length. A size series of ten individuals ranging from 32 to 210mm standard length (0.7–158.6g body mass) was collected from Bevis Pond, Leon County, Florida, USA. The fish were housed separately in 30 or 100l aquaria at 20–21°C. The bass were trained to feed on live mollies (*Poecilia latipinna*) held by forceps, with camera lights on. In order to minimize prey-size effects on prey capture (Werner, 1974), only mollies with a body diameter of 40–60% of bass mouth gape were used for videotaping. Thus, the size of prey used increased with increasing size of the bass. Feeding sequences were videotaped using a single-camera NAC HSV-400 high-speed video system with synchronized strobe at 200 fields s⁻¹, in lateral view with a 1cm grid background. Prey capture events were recorded over a period of 2–12 days for each bass until ten sequences appearing to be of maximal predator effort were obtained. We deemed feeding sequences to represent maximal predator effort if they appeared to be very explosive in nature, with feeding apparatus displacements at their apparent extremes, such as the attainment of maximum gape. Only those feedings in which the largemouth bass was estimated as being in full lateral view throughout the feeding event were considered acceptable for analysis. After the desired number of feedings had been recorded, each bass was killed in a solution of MS-222 (tricaine methanesulfonate), standard length was measured and the specimen was fixed in 10% formalin for later morphological measurements.

Video analysis

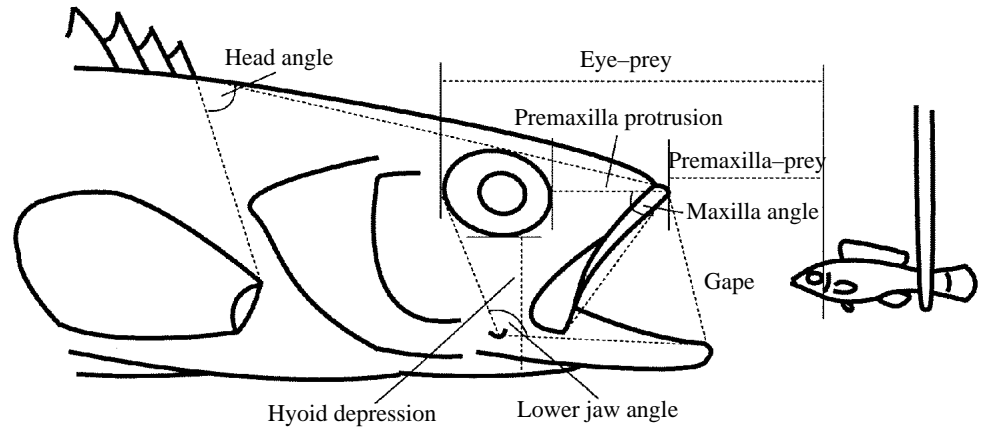
One hundred prey-capture sequences (10 per bass) were analyzed field-by-field using Measurement TV software (Updegraff, 1990). Eight variables were measured from every field of the entire gape cycle of all sequences. For this study, the 'gape cycle' was defined as the events occurring between time zero and the field where the prey was seized between the jaw tips. 'Time zero' was the field immediately preceding the field containing the first movement of the lower jaw tip beginning jaw depression. The eight variables consisted of five

linear distances and three angles, which quantified movements of the head, jaws, hyoid and body (Fig. 1). Gape was the distance from the anterior tip of the premaxilla to the anterior tip of the mandible and was a measure of mouth opening distance. Premaxilla protrusion was the perpendicular distance between two vertical lines, one at the anterior-most point of the eye and the other at the tip of the premaxilla, and was a measure of the forward protrusion of the mouth during prey capture. Hyoid depression was the perpendicular distance between a line at the ventral-most point of the eye and the most ventral point of the floor of the mouth, which indicated the extent of buccal cavity expansion during feeding. Predator eye to prey distance was the perpendicular distance between two vertical lines, one at the posterior-most point of the predator's eye and the other placed at the posterior-most point of the eye of the prey. Premaxilla to prey distance was the perpendicular distance between vertical lines at the tip of the predator's premaxilla and the posterior-most point of the eye of the prey. Eye to prey distance was used to calculate predator approach velocity and premaxilla to prey distance was used to determine the added velocity of jaw protrusion during prey capture. Head angle was the angle between a line from the first dorsal fin spine to the dorsal tip of the rostrum and a line from the first dorsal fin spine to the origin of the first pectoral fin ray and was used to determine the extent of cranial elevation, which often contributed to increasing mouth gape during feeding. Lower jaw angle was the angle between a line from the jaw hinge to the posterior-most point of the eye and a line from the jaw hinge to the anterior tip of the mandible; it was used to calculate the velocity of movement of the mandible during mouth opening and closing. Maxilla angle was measured as the angle between two lines, one passing from the anterior tip of the premaxilla to the anterior-most point of the eye and the other from the tip of the premaxilla to the anteroventral head of the maxilla and was an additional measure of jaw movement.

Quantifying kinematics

Plots of each kinematic variable against time were generated for all prey capture sequences, yielding a total of 800 kinematic profiles. An additional 14 variables, which quantified the magnitude and timing of movements during prey capture, were calculated from the kinematic profiles. The maximum linear displacements were determined for gape, premaxillary protrusion and hyoid depression. The maximum angular displacements were calculated for head angle, lower jaw angle and maxilla angle. The angular displacements were standardized by subtracting the magnitude at 'time zero' from all measurements so that the angular displacement at 'time zero' would be equal to zero. Six variables quantified the time to maximum displacement or peak (measured from time zero) for gape, premaxillary protrusion, hyoid depression, cranial elevation, maxilla rotation and lower jaw depression. Another variable, duration of lower jaw adduction, was calculated as the time from peak lower jaw depression to lower jaw contact with the prey. Gape cycle time, from time zero to prey contact,

Fig. 1. Lateral schematic view of a largemouth bass at the midpoint of the gape cycle illustrating the eight kinematic variables measured from every field of the entire gape cycle of all prey-capture sequences. Three variables quantifying linear displacements of the feeding apparatus were measured: gape, hyoid depression and premaxilla protrusion. Three variables quantifying angular displacements of the feeding apparatus were measured: head angle, lower jaw angle and maxilla angle. Two additional linear displacements were measured to quantify the movement of the bass toward the prey: eye-prey distance and premaxilla-prey distance. See text for detailed descriptions of the kinematic variable measurements



was calculated for all prey-capture sequences. The gape cycle was further analyzed by plotting the percentage of the gape cycle devoted to mouth opening against standard length. The displacement records for the initial eight kinematic variables were also used to generate velocity profiles for the eight variables, by dividing the displacement between successive fields by the 5ms interval between fields. From the 800 velocity profiles, 10 additional variables were determined which quantified the maximal linear and angular velocities of movements, for each prey capture sequence. Maximal linear velocities of hyoid depression, premaxillary protrusion, gape opening and closing and both eye-prey and premaxilla-prey approach velocities were calculated. Maximal angular velocities were calculated for cranial elevation, maxilla rotation and lower jaw depression and adduction. The maximal velocities were determined by taking the single greatest displacement from the velocity profiles, which usually occurred immediately preceding peak gape for opening movements and immediately following peak gape for closing movements.

Scaling kinematic variables

In total, 240 kinematic variable measurements were made for each of the ten individuals used in the study (24 variables \times 10 prey-capture sequences). Means were calculated for each individual for all 24 variables. The means were \log_{10} -transformed and then plotted against the \log_{10} of standard length for all individuals. Least-squares regressions were fitted to all variable plots to determine scaling exponents and y-intercepts. We chose least squares, instead of alternative regression models, because our main objective was to determine whether standard length affects the kinematics of prey capture rather than to describe the nature of the relationship between variables (Ricker, 1973). The observed scaling relationships were compared with those expected under two models of geometric similarity using Student's *t*-tests with Bonferroni-corrected probability values. Our major goal in this analysis was to compare the overall performance of the two

models in predicting the scaling of kinematic variables. We chose to use Bonferroni-corrected probability values to minimize the number of times significant differences between the models and our data were found when there was, in fact, no significant difference. All statistical calculations were performed using SYSTAT for Windows, Version 5 (Wilkinson, 1992).

Scaling morphology

The potential of size-induced changes in mechanics of the feeding mechanism was investigated by examining the lever arms of the lower jaw and the size and shape of selected cranial muscles. The left mandible was dissected from each of the ten study specimens and linear measurements of the lever arms of the lower jaw were made using a Wild M5A dissecting microscope with an ocular micrometer. Three lever arm measurements were made: the jaw opening in-lever was measured from the jaw articulation to the attachment of the interoperculo-mandibular ligament; the jaw closing in-lever was measured from the jaw articulation to the insertion of the adductor mandibulae muscle within the lower jaw; and the out-lever for jaw opening and closing was taken as the distance from the jaw articulation to the anterior tip of the mandible (Fig. 2A). The actual in-levers, from the jaw hinge to the insertion of the force-transmitting ligaments, were measured rather than attempting to measure the effective in-levers (the distance to a point that is perpendicular to the driving force vector) which, in a dynamic system such as this, change throughout a 60° rotation of the lower jaw. It should be noted that the actual in-levers for both opening and closing do approach or pass through a 90° angle with respect to the driving force vector at some point in the rotation of the lower jaw. The lever arm measurements for all individuals were \log_{10} -transformed and plotted against the \log_{10} of standard length for all individuals, and regressions were calculated to determine the scaling relationships for the lever arms of the lower jaw.

Possible changes in mechanical advantage were investigated

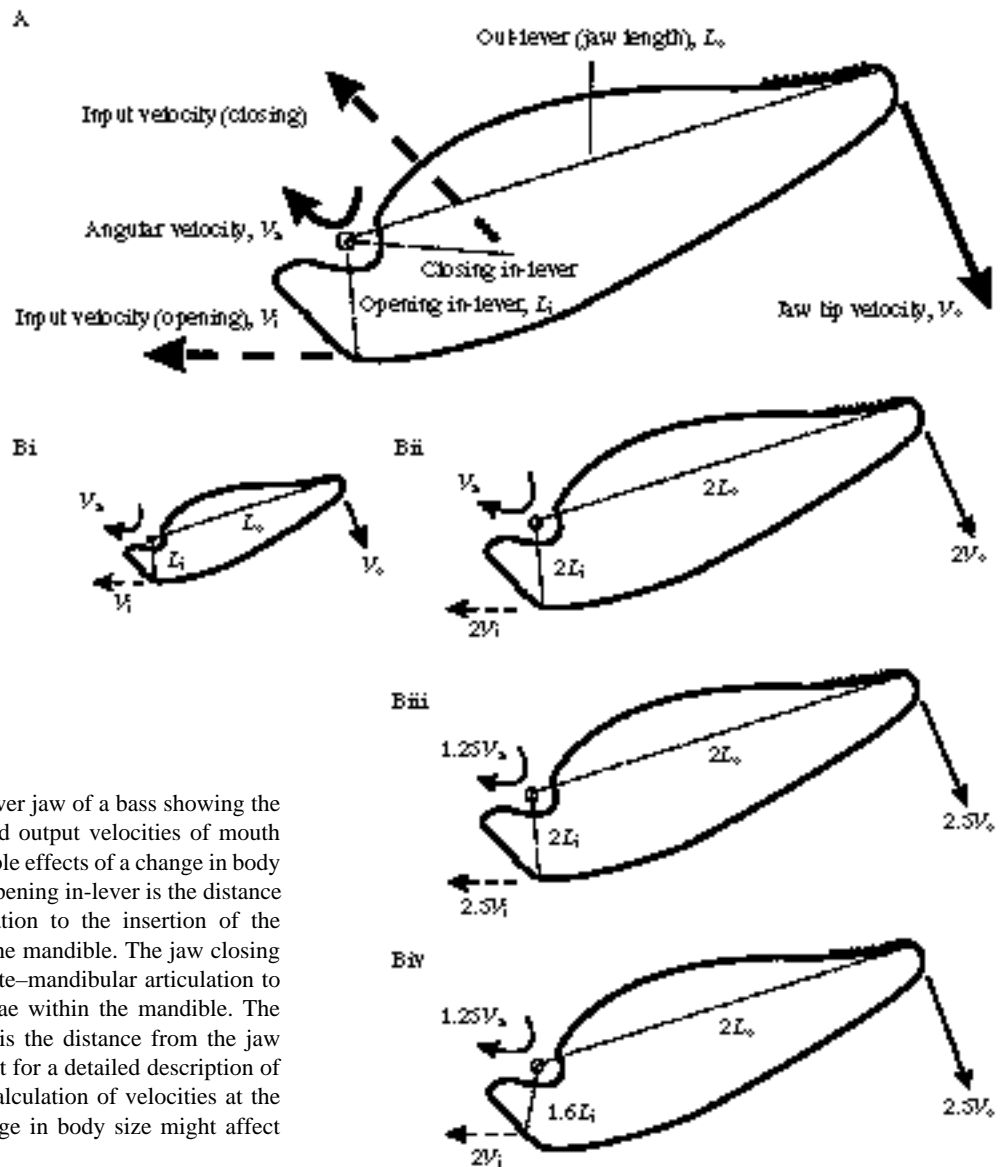


Fig. 2. Schematic illustrations of the lower jaw of a bass showing the lever arms of the jaw and the input and output velocities of mouth opening and closing (A) and three possible effects of a change in body size on kinematic output (B). The jaw opening in-lever is the distance from the quadrato-mandibular articulation to the insertion of the interoperculo-mandibular ligament on the mandible. The jaw closing in-lever is the distance from the quadrato-mandibular articulation to the insertion of the adductor mandibulae within the mandible. The out-lever for jaw opening and closing is the distance from the jaw hinge to the tip of the mandible. See text for a detailed description of the mechanical model explaining the calculation of velocities at the jaw tip and jaw hinge and how a change in body size might affect output velocities.

by calculating and plotting the lever arm ratios for jaw opening and closing against standard length. The ratios were calculated by dividing the opening and closing in-lever distances by the out-lever for each individual. The in-lever to out-lever ratios for lower jaw opening and closing are indicative of the trade-off between velocity and force transmission at the jaw tip. High in-lever to out-lever ratios result in high force transmission at the end of the out-lever, whereas lower ratios produce greater velocity (Barel, 1983; Wainwright and Richard, 1995). Regressions were calculated for the opening and closing lever-arm ratio plots. Both the lever arm scaling relationships and lever arm ratios were tested against geometric similarity, using Student's *t*-tests with Bonferroni-corrected probability values.

Additionally, the mass and shape of the two major muscles that drive the feeding mechanism were quantified. The sternohyoideus, the major muscle driving lower jaw depression, and the adductor mandibulae, the muscle responsible for lower jaw adduction, were dissected from each

of the ten largemouth bass. The entire sternohyoideus was dissected from each individual and the left-side adductor mandibulae complex was removed from each fish. Each muscle was weighed twice on a Mettler AJ100 balance to the nearest 0.001g and the mean for the two measurements was taken as the mass of each muscle for each individual. A series of linear measurements was made on all muscles to quantify the shape of each muscle for each fish. Three linear measurements were made on the sternohyoideus muscle: (1) the length was measured as the distance from the urohyal to the pectoral girdle along the ventral aspect of the muscle; (2) the midlength width was measured as the distance perpendicular to the length at the midpoint of the length measurement; and (3) the pectoral girdle width was measured as the distance perpendicular to the length at the pectoral girdle origin. Three linear measurements were also made on the adductor mandibulae complex: (1) dorsal length was measured as the distance from the insertion on the mandible along the

dorsal aspect to the posterodorsal origin; (2) midline length was measured as the distance from the insertion on the mandible to the posterior point of origin at the midpoint between the most posterior dorsal and ventral origins; and (3) adductor mandibulae thickness was measured as the greatest width of the muscle when viewed from the dorsal aspect, which was typically at the overall midpoint of the muscle. The muscle masses and lengths were \log_{10} -transformed and plotted against the \log_{10} of standard length for all individuals, and regressions were calculated to determine the scaling relationships for these two major muscles that drive the feeding mechanism. The effect of changing mass of the mandible was also investigated by dissecting out the left mandible from each bass and weighing it twice and then regressing the \log_{10} -transformed mean value against the \log_{10} of standard length to determine the scaling relationship for lower jaw mass. The scaling relationship for body mass was also determined by regressing \log_{10} -transformed body masses against the \log_{10} of standard length.

Two models of kinematic scaling

The lower jaw of *Micropterus salmoides* can be modeled as a simple lever system to investigate possible effects of scale on the mechanical basis of kinematics. A mechanical model of the lower jaw of a fish can be used to predict how the kinematic output of mouth opening and closing might be expected to change with increasing body size (Fig. 2A). Given an input velocity acting on the in-lever causing rotation of the out-lever, one can calculate the jaw tip velocity and angular velocity about the jaw hinge using two simple formulae: (1) the resultant jaw tip velocity (V_o) is the product of the input velocity (V_i) and the ratio of the out-lever (L_o) to the in-lever (L_i); thus, $V_o = V_i(L_o/L_i)$; and (2) the resultant angular velocity (V_a) is proportional to the ratio of the input velocity (V_i) to the in-lever (L_i), and thus $V_a \propto V_i/L_i$.

In a consideration of how change in body size might affect jaw movements, we will first take into account the input velocity from the above formulae. The input velocity is determined predominantly by the contraction velocity of the muscle or muscles driving the movements. Muscle contraction velocity is a function of the rate of shortening of each sarcomere and the number of sarcomeres in series for the muscle. Assuming that sarcomere length is constant within a muscle during ontogeny, one can then predict that, if a muscle were to maintain a constant shape and architecture with increasing size, the overall muscle shortening velocity, under unloaded conditions, would increase by the multiple of its increase in length. For example, a muscle of length X will have a maximum shortening velocity of V , and a muscle of the same shape of length $10X$ will have a maximum shortening velocity of $10V$.

A schematic diagram of three possible effects of change in body size on kinematic output is shown in Fig. 2B. On the left (Fig. 2Bi) is shown the initial stage with input velocity of V_i , in-lever length of L_i , out-lever length of L_o , and the resultant jaw tip velocity of V_o and angular velocity at the jaw

articulation of V_a . In Fig. 2Bii, an example of the expected changes in kinematic output is illustrated, given the maintenance of geometric similarity (constant shape) with a doubling in size. The input velocity is increased to $2V_i$, the in-lever has length $2L_i$, the out-lever has length $2L_o$, and the resulting jaw tip velocity increases to $2V_o$ while the angular velocity at the jaw articulation remains V_a . In Fig. 2Biii, we see one result of a deviation from geometric similarity in which the input velocity of muscular contraction increases to $2.5V_i$, while the lever arms of the jaw simply double in length as above. In this case, the increase in input velocity results in an increase in jaw tip velocity to $2.5V_o$ and an angular velocity at the jaw hinge of $1.25V_a$. A similar result can be effected by keeping the input velocity at $2V_i$, but shortening the in-lever to $1.6L_i$ as shown in Fig. 2Biv, which also results in an increase in jaw tip velocity to $2.5V_o$ and an increase in angular velocity to $1.25V_a$.

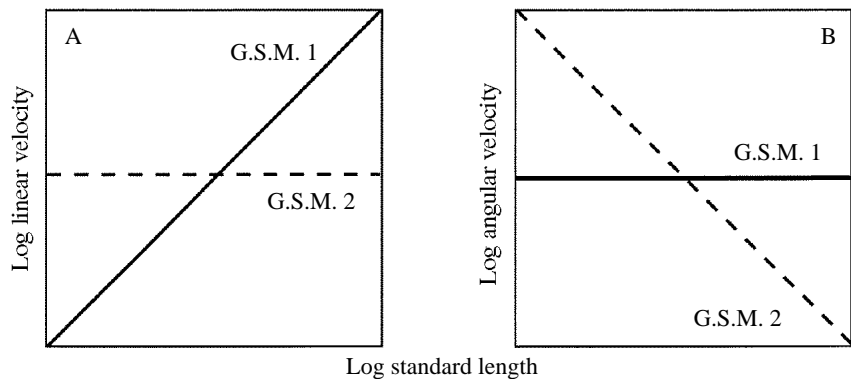
The effects of change in body size on kinematic output, given the maintenance of constant proportions (isometry) of the feeding mechanism and a proportional increase of input velocities, are plotted for linear and angular velocities (Fig. 3). The figure shows that when plotting \log_{10} -transformed linear and angular velocities against the \log_{10} of standard length, one expects to see scaling relationships with a slope of 1 for linear velocities and a slope of 0 for angular velocities.

A second approach to modeling expected scaling relationships is that of Hill (1950) and O'Reilly *et al.* (1993). Following different lines of reasoning, these authors predict the same scaling pattern for kinematics. For example, the O'Reilly *et al.* (1993) approach focuses on the ability of a muscle to accelerate the mass of a structure. Thus, the model takes into account the differential scaling of the cross-sectional area of muscle and body mass. If geometric similarity is maintained, then the cross-sectional area of muscle, or force-producing capability, would be expected to increase as the square of body length, and body mass or the mass of any component of the body would be expected to increase as the cube of body length. This model predicts that, as body size increases, force production of the muscles powering movements would increase at a slower rate than the mass of the components being moved. The effects of change in body size on kinematic output predicted by the above model are also plotted for linear and angular velocities (Fig. 3). This model would predict that, when plotting \log_{10} -transformed linear and angular velocities against the \log_{10} of standard length, linear velocities would scale with a slope of 0 and angular velocities would scale with a slope of -1 .

Both models allow for predictions of the timings of movements, such as time to peak gape or time to peak head angle. This is possible because each model allows the calculation of an expected maximal velocity for an animal of a given size. Thus, given a feeding apparatus movement of a given distance (linear or angular) and an expected maximal velocity for that movement, one can solve for the expected time to make the movement by dividing the displacement distance by the expected velocity.

The two models of geometric similarity were used to

Fig. 3. Two \log_{10}/\log_{10} plots showing the effects of change in body size on kinematic output, given the maintenance of constant proportions (isometry) for linear and angular velocities under two different models. Under our geometric similarity model (G.S.M. 1), linear velocities would be expected to increase in direct proportion to body size and angular velocities would be expected to remain constant with increasing body size. Under the second geometric similarity model (G.S.M. 2) of Hill (1950) and O'Reilly *et al.* (1993), linear velocities would be expected to remain constant and angular velocities would be expected to be inversely proportional to body size as body size increases.



determine the expected scaling relationships for the 24 kinematic variables, given constancy of shape with increase in body size. Using our model, the following scaling relationships would be expected: linear displacements would scale with a slope of 1 and angular displacements with a slope of 0, time-to-peak variables and gape cycle time would scale with a slope of 0, maximal linear velocities would scale with a slope of 1 and maximal angular velocities would scale with a slope of 0. The alternative model of Hill (1950) and O'Reilly *et al.* (1993) would give the following scaling expectations: linear and angular displacements would scale as above, time-to-peak variables and gape cycle time would scale with a slope of 1, maximal linear velocities would scale with a slope of 0 and maximal angular velocities would scale with a slope of -1 . The expected scaling relationships from both models were used as a basis for comparison with the observed scaling relationships for all variables.

Results

The typical prey-capture sequence for *Micropterus salmoides* is characterized by the following patterns of movement of the feeding apparatus. As the bass approaches the prey, there is simultaneous elevation of the head, depression of the hyoid apparatus and depression of the lower jaw. As the lower jaw depresses, there is a corresponding anterior rotation of the maxilla and protrusion of the premaxilla. Maximum gape is usually achieved when movements of the head, hyoid, lower jaw, maxilla and premaxilla all reach their peak displacements. Mouth closing is usually initiated when the prey is within the plane between the upper and lower jaw tips and is characterized by the simultaneous adduction of the lower jaw and ventral flexion of the head, followed by posterior rotation of the maxilla, posterior movement of the premaxilla and dorsal movement of the hyoid, culminating in the grasping of the prey between the jaw tips.

Representative kinematic profiles of prey capture from two largemouth bass, of 33mm and 201mm standard length, are presented in Fig. 4. The profiles show movement records for gape distance, hyoid depression, lower jaw angle and head angle for both fish on the same time scale, beginning with the

field preceding time zero and ending with prey contact. It should be noted from the gape and hyoid profiles that the time taken to reach peak gape and maximum hyoid depression was considerably longer in the larger bass. The 33mm bass reached its peak gape of 9mm in 20ms, whereas the 201mm bass took 40ms to reach its peak gape of 40mm. The jaw angle and head angle profiles indicate that the angular displacements are nearly identical for both fish, but the time course of the angular displacements was of considerably longer duration in the larger fish. For example, the small bass achieved a maximum head angle displacement of 30° in a time of 20ms, whereas the larger bass reached its maximum head angle displacement, also of 30° , in a longer time of 40ms.

Scaling displacements

All linear and angular displacements scaled isometrically such that all linear excursion distances increased with increasing body size, as expected given geometric similarity, and all angular displacements remained constant regardless of body size (Table 1; Fig. 5). Maximum gape distance, maximum hyoid depression and maximum premaxillary protrusion all scaled with slopes that were not significantly different from 1 (Fig. 5A). The scaling relationships of the angular displacements of the lower jaw, head and maxilla all had slopes equal to zero, indicating that the magnitude of angular displacements was unaffected by body size (Fig. 5B).

Scaling time

All timing variables showed increases in duration with increasing body size (Table 1; Fig. 6). Time to peak gape and time to peak hyoid depression had slopes significantly different from 0, indicating that it took longer to reach peak gape and maximum hyoid depression in larger fish (Fig. 6A). Of the angular displacements, duration of lower jaw adduction was significantly different from 0; thus, larger fish closed their mouth more slowly than did the smaller fish. Times to peak head angle, lower jaw depression and maxilla rotation also tended to increase with size, but were not significantly different from zero at the very conservative P -value of 0.002 (Fig. 6B). Even though the angular displacements were roughly the same

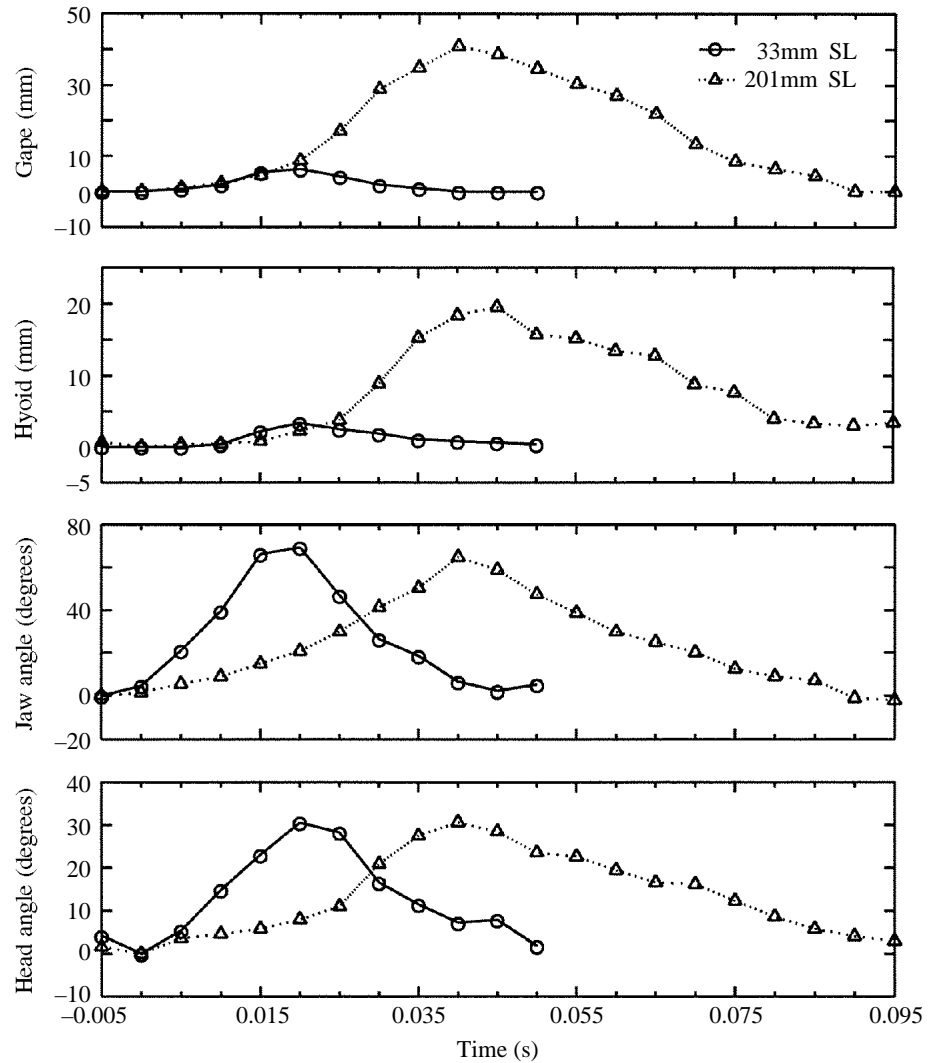


Fig. 4. Representative kinematic profiles of prey capture of two largemouth bass of different body size plotted together on the same time scale. Profiles are presented for two linear displacements, gape and hyoid depression, and two angular displacements, lower jaw angle and head angle. Note that the linear displacements increase in both magnitude and duration in the larger bass, whereas the angular displacements are nearly equal, but of longer duration, in the larger bass.

for all individuals, the time taken to complete the movements became considerably longer with increasing body size.

Gape cycle time increased substantially in larger bass, differing significantly from a slope of 0, indicating a significant change in gape cycle time with increase in body size (Fig. 7). A bass of 33 mm had an average gape cycle time of 37 ms, whereas a bass of 201 mm had an average gape cycle time of 80 ms (Fig. 7A). The examination of the percentage of the gape cycle devoted to mouth opening revealed a trend indicating that mouth opening accounts for more than 50% of the gape cycle in bass less than 100 mm SL (55–65%), but it accounts for 50% or less of the gape cycle (42–50%) in the larger bass (Fig. 7B). Thus, not only did total gape cycle time increase, but the proportion of the gape cycle made up by mouth opening or closing changed with increasing size.

Scaling velocities

The scaling relationships of maximal linear and angular velocities for all variables showed a pattern in which linear velocities became faster with increasing body size and

angular velocities became slower with increasing body size (Table 1; Fig. 8). Maximum jaw tip velocity of closing and premaxillary protrusion velocity slopes were significantly less than 1, indicating a relative slowing of maximal jaw tip closing and premaxillary protrusion velocities with increasing size. Maximal jaw tip velocity of opening and maximal hyoid depression velocity slopes were not significantly different from 1 under the conservative P -value of 0.002 (Fig. 8A). The maximal angular velocity slopes for cranial elevation, lower jaw depression and lower jaw adduction all had slopes significantly different from zero, revealing a distinct decrease in angular velocities with increasing bass size (Fig. 8B).

The predator approach velocities, in contrast to those of the feeding mechanism, scaled isometrically. Both predator body-to-prey and predator mouth-to-prey maximal velocities scaled with slopes of approximately 1, indicating a proportional increase in approach velocity with increase in body size. Maximum approach velocity was more rapid with increasing body size (Fig. 9).

Table 1. *Scaling relationships for 24 variables measured from kinematic profiles of a size series of ten largemouth bass Micropterus salmoides*

Variable	G.S.M. 1 slope	G.S.M. 2 slope	Least square		y-intercept	S.E.M.	r^2	t	
			slope	S.E.M.				(G.S.M. 1)	(G.S.M. 2)
Maximum gape	1	1	1.10	0.08	-0.98	0.16	0.96	1.2	1.2
Maximum premaxillary protrusion	1	1	0.93	0.02	-0.61	0.03	0.99	-3.9	-3.9
Maximum hyoid depression	1	1	1.19	0.06	-1.12	0.11	0.98	3.3	3.3
Head angle displacement	0	0	-0.01	0.06	1.42	0.12	0.00	-0.1	-0.1
Jaw angle displacement	0	0	0.01	0.06	1.77	0.11	0.01	0.2	0.2
Maxilla angle displacement	0	0	0.05	0.05	1.59	0.11	0.08	0.8	0.8
Time to peak gape	0	1	0.31	0.07	-2.12	0.14	0.71	4.5*	-9.8*
Time to peak premaxillary protrusion	0	1	0.21	0.08	-1.94	0.17	0.44	2.5	-9.3*
Time to peak hyoid depression	0	1	0.31	0.06	-2.09	0.12	0.78	5.3*	-11.9*
Time to peak cranial elevation	0	1	0.30	0.07	-2.08	0.14	0.70	4.3	-10.2*
Time to peak lower jaw depression	0	1	0.30	0.07	-2.09	0.14	0.69	4.3	-10.0*
Duration of lower jaw adduction	0	1	0.58	0.09	-2.73	0.19	0.83	6.3*	-4.5*
Time to peak maxilla rotation	0	1	0.30	0.07	-2.09	0.15	0.67	4.0	-9.5*
Gape cycle time	0	1	0.43	0.07	-2.09	0.14	0.83	6.1*	-8.1*
Maximum jaw tip velocity of opening	1	0	0.76	0.09	-1.45	0.17	0.91	-2.8	8.8*
Maximum jaw tip velocity of closing	1	0	0.64	0.05	-1.23	0.10	0.95	-7.0*	12.2*
Maximum velocity of premaxillary protrusion	1	0	0.39	0.08	-1.44	0.15	0.77	-7.9*	5.1*
Maximum velocity of hyoid depression	1	0	0.75	0.10	-1.70	0.20	0.87	-2.5	7.5*
Maximum angular velocity of cranial elevation	0	-1	-0.24	0.05	1.96	0.09	0.77	-5.3*	16.5*
Maximum angular velocity of lower jaw depression	0	-1	-0.33	0.07	2.41	0.13	0.75	-4.9*	10.2*
Maximum angular velocity of lower jaw adduction	0	-1	-0.50	0.07	2.84	0.13	0.87	-7.5*	7.4*
Maximum angular velocity of maxilla rotation	0	-1	-0.15	0.08	2.11	0.16	0.29	-1.8	10.5*
Maximum approach velocity (eye-prey)	1	0	0.89	0.16	-1.88	0.33	0.79	-0.7	5.4*
Maximum approach velocity (mouth-prey)	1	0	0.84	0.16	-1.72	0.32	0.77	-1.0	5.2*

All statistics were calculated on \log_{10} -transformed variables.

The t -tests compare the observed least squares slopes to the slopes of the G.S.M. 1 and G.S.M. 2 models.

Asterisks next to t -values denote significance at the Bonferroni columnwise corrected P -value of 0.002.

G.S.M. 1, geometric similarity model of the authors.

G.S.M. 2, geometric similarity model of Hill (1950) and O'Reilly *et al.* (1993).

Scaling lower jaw mechanics

The morphological analysis of the lever arms of the lower jaw revealed that all aspects of the lever arm system scaled isometrically, indicating that geometric similarity was maintained in the mechanics of the lower jaw (Table 2; Fig. 10). The opening and closing in-levers as well as jaw length scaled with slopes indistinguishable from 1 (Fig. 10A). The examination of lever arm ratios for jaw opening and closing show that the lever arm ratios remain constant throughout the size series (Fig. 10B). The constancy of the lever arm ratios indicates that there is no change in mechanical advantage of the jaw opening and closing systems with changes in body size.

The analysis of the scaling of muscle morphology also revealed that the two major muscles of the feeding mechanism scaled isometrically with respect to mass and shape. The measurements of mass for the adductor mandibulae complex and the sternohyoideus scaled with slopes not significantly different from 3, which indicates the maintenance of geometric

similarity with respect to mass (Table 2). The two measurements of shape for the adductor mandibulae complex that quantified muscle length scaled with slopes approximately equal to 1, indicating no significant change in length of the adductor mandibulae complex with increasing bass size. The measurement of adductor mandibulae thickness scaled with a slope of 1.22, suggesting that the adductor mandibulae became relatively thicker with increasing size, though the slope was not significantly different from 1 (Table 2). All three measurements of shape for the sternohyoideus scaled with slopes approximately equal to 1, indicating no significant change in the shape of this muscle with increasing size during ontogeny (Table 2).

In addition, the mass of the mandible scaled with a slope approximately equal to 3, indicating isometry with respect to standard length. Thus, the mass of the lower jaw remained relatively constant with increasing body size. Body mass also scaled isometrically in our size series of largemouth bass (Table 2).

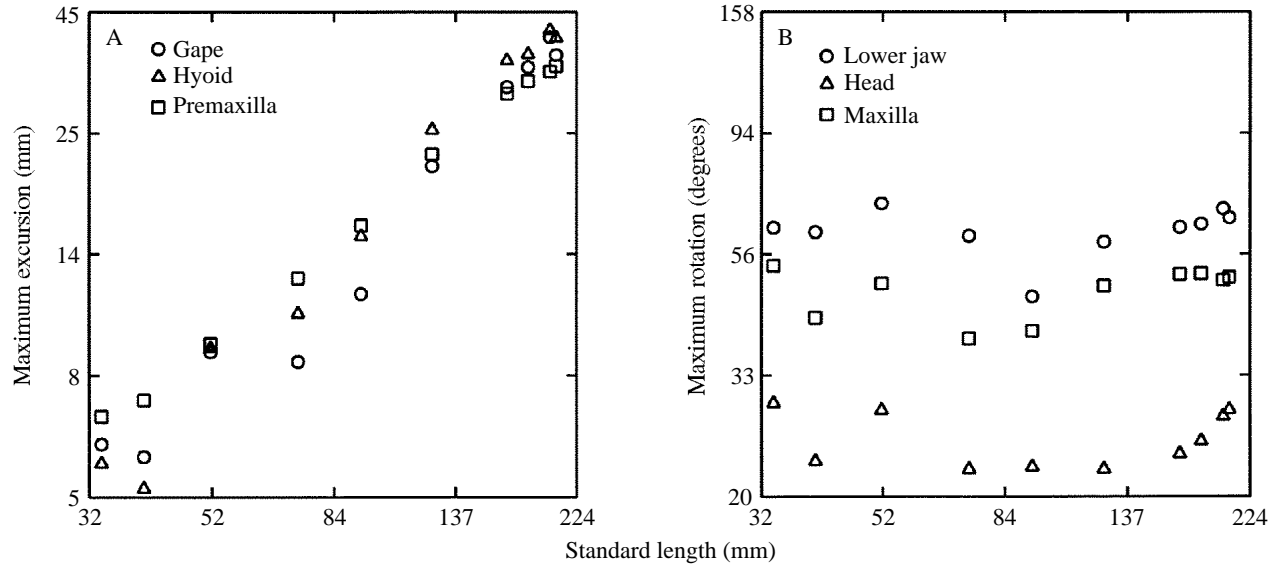


Fig. 5. \log_{10}/\log_{10} scatterplots of the mean maximum value of six kinematic variables against standard length for ten largemouth bass. Note that the maximum excursion distances increase in proportion to body size (A) and that the maximum rotations remain relatively constant with increasing body size (B).

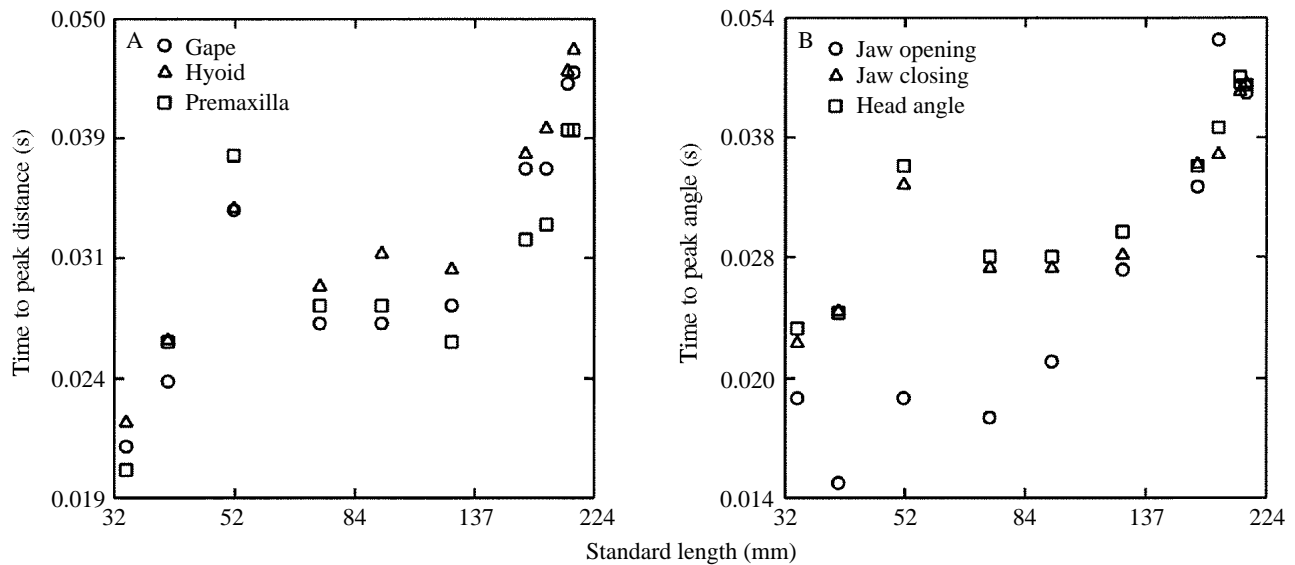


Fig. 6. \log_{10}/\log_{10} scatterplots of the mean time to peak distance of six kinematic variables against standard length for ten largemouth bass. Note that all timing variables show a trend of increasing duration with increasing body size.

Comparison with the models

The observed scaling relationships for all 24 kinematic variables were compared with expected scaling relationships under the two different models of kinematic scaling (Table 1). Both models predicted that linear displacements would increase in proportion to body size and that angular displacements would remain constant. The observed scaling relationships for both linear and angular displacements were not significantly different from the expectations of the models. A comparison of timing variables revealed that four of the eight variables differed significantly from the expectations of our model, but all eight variables were significantly different from those of the

alternative model. The comparison of linear velocities found that two of the six variables differed significantly from our model, but all six variables were significantly different from the expectations of the alternative model. Three of the four angular velocity variables were significantly different from our model and all four angular velocity variables differed significantly from the alternative model.

Discussion

The results of this study indicate that body size had significant effects on the kinematics of prey capture in the

Table 2. Scaling relationships for 15 morphological variables measured from a size series of ten largemouth bass *Micropterus salmoides*

Variable	Isometry slope	Least squares slope	S.E.M.	y-intercept	S.E.M.	r^2	t (LS)
Opening in-lever of the lower jaw	1	1.00	0.04	-1.55	0.08	0.99	0.1
Closing in-lever of the lower jaw	1	1.01	0.03	-1.48	0.06	0.99	0.3
Jaw length (out-lever for opening and closing)	1	1.07	0.02	-0.89	0.05	0.99	2.8
Jaw opening lever arm ratio	0	0.00	0.00	0.18	0.01	0.17	0.0
Jaw closing lever arm ratio	0	0.00	0.00	0.21	0.00	0.47	0.0
Body mass	3	2.94	0.04	-4.61	0.08	0.99	-1.5
Adductor mandibulae mass	3	3.05	0.07	-7.09	0.14	0.99	0.7
Sternohyoideus mass	3	2.84	0.10	-6.37	0.20	0.99	-1.6
Lower jaw mass	3	3.06	0.05	-7.10	0.10	0.99	1.2
Adductor mandibulae length (dorsal aspect)	1	0.94	0.02	-0.81	0.03	0.99	-3.0
Adductor mandibulae length (midline)	1	1.02	0.02	-0.99	0.04	0.99	1.0
Adductor mandibulae thickness	1	1.22	0.08	-2.11	0.15	0.97	2.7
Sternohyoideus length	1	0.92	0.04	-0.74	0.08	0.98	-2.0
Sternohyoideus width (midlength)	1	0.89	0.04	-1.17	0.08	0.98	-2.7
Sternohyoideus width (pectoral girdle)	1	1.03	0.05	-1.13	0.09	0.99	0.6

All statistics were calculated on \log_{10} -transformed variables, except those involving ratios, which were calculated on untransformed variable values.

The t -tests compare the observed least squares slopes to those expected under isometry, where body proportions remain constant with increasing size.

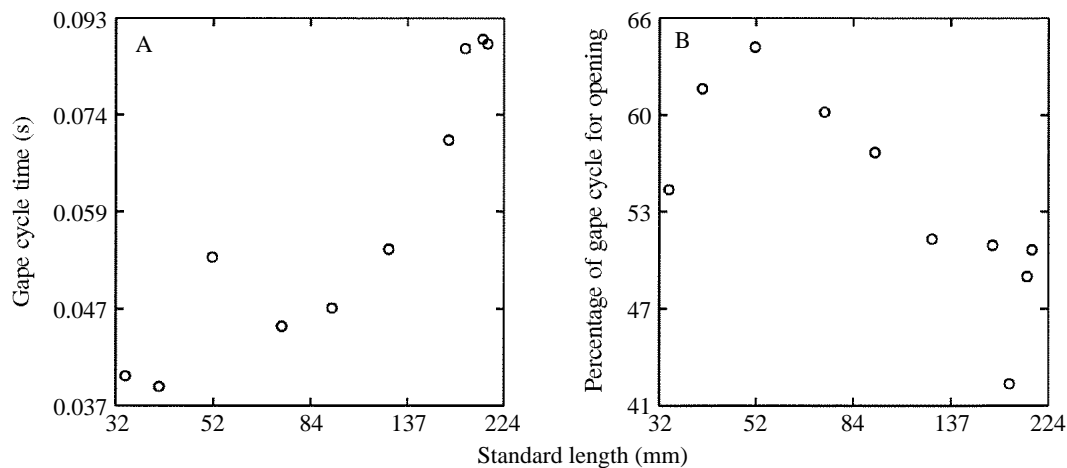


Fig. 7. \log_{10}/\log_{10} scatterplot of mean gape cycle time for ten largemouth bass (A) and a scatterplot of the percentage of the gape cycle devoted to mouth opening for the ten bass (B), both plotted against standard length. Note the significant increase in total gape cycle time with increasing body size and the change in the amount of time devoted to mouth opening with change in body size.

largemouth bass. Smaller bass opened and closed their mouths more rapidly than larger bass. The linear displacements of the feeding apparatus scaled in direct proportion to body size and angular displacements remained constant with increasing body size, indicating isometry of movements. However, the timings and velocities of those movements changed significantly with body size. The times to peak displacement increased in duration with increasing body size. The linear velocities of displacements were relatively slower with increasing size and the angular velocities of feeding mechanism displacements were absolutely slower with increasing size. Thus, while

feeding mechanism displacements were of the same magnitude regardless of body size, the timings and velocities of those movements were strongly affected by body size.

The results of this study do not appear to be in accordance with the models of the scaling of musculo-skeletal systems considered in this paper. Our results for timings and velocities of feeding mechanism movements were significantly different from our simple scaling model, which incorporated unloaded muscle contraction velocities. The results are in even greater discord with an alternative model of the scaling of feeding kinematics (Hill, 1950; O'Reilly *et al.* 1993). The scaling

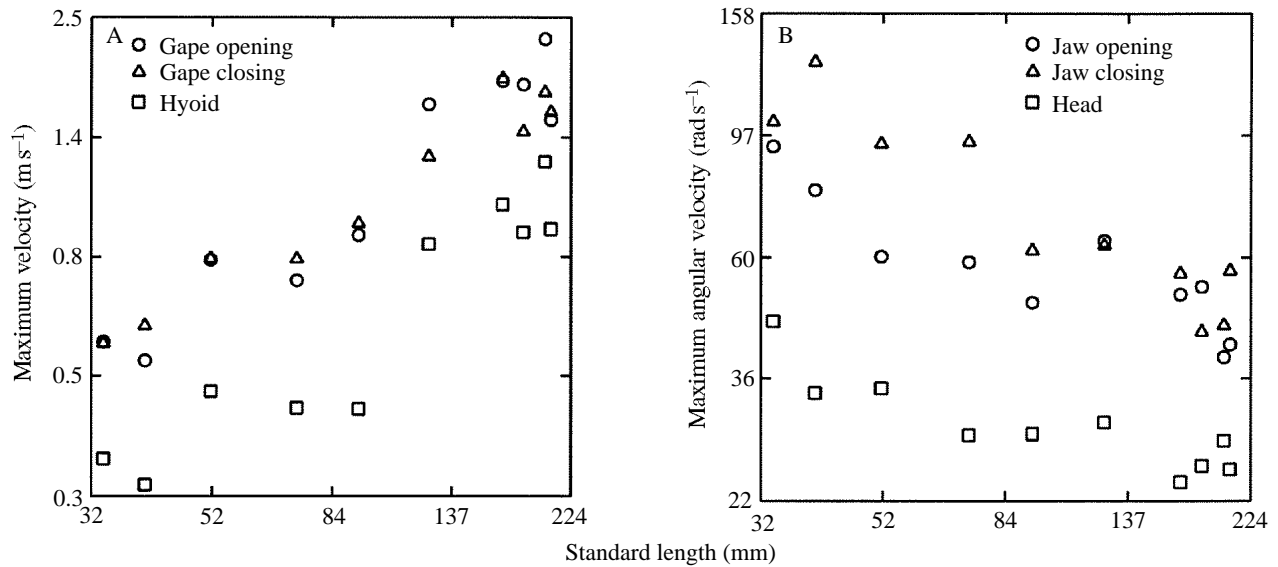


Fig. 8. \log_{10}/\log_{10} scatterplots of mean maximal velocities of six kinematic variables against standard length for ten largemouth bass. Note that maximum linear velocities increase with body size (A), whereas maximum angular velocities decrease with increasing body size (B).

relationships observed for the largemouth bass were significantly different from the expectations of our model for half of the timing and velocity variables and were significantly different from the alternative model expectations for all 18 variables. Thus, our results indicate that the scaling of prey capture kinematics is not readily explained by these models of the effects of body size on feeding kinematics.

Theoretical basis of kinematic allometry

Our simple mechanical model of the isometric scaling of prey capture kinematics was founded on two basic assumptions. The first assumption was that the lever arms of the lower jaw would themselves scale in an isometric fashion and that the mechanical advantage of opening and closing of the lower jaw would remain constant regardless of body size. The second assumption, that muscle shortening velocity would be proportional to standard length, was based on the expectation that unloaded muscle contraction velocities would scale in direct proportion to body size.

One possible explanation for changes in prey-capture kinematics with increasing size could have been a change in the scaling of the lever arms of the lower jaw, resulting in changes in mechanical advantage of the feeding apparatus and thereby altering kinematic output. Our examination of the scaling of the jaw levers revealed that the lever arms of the lower jaw scaled isometrically, and that there was no change in mechanical advantage with change in body size. In addition, our examination of the scaling of the two major muscles involved in jaw opening and closing revealed that these muscles scaled isometrically with respect to mass and shape and that lower jaw mass also scaled isometrically. Thus, the deviation of the observed kinematic scaling from our model must be attributed to deviations from our expected scaling of contractile speed of the muscles powering the feeding

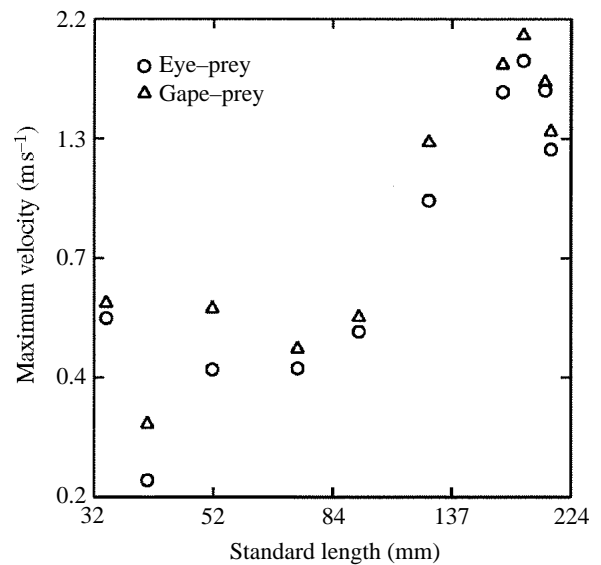


Fig. 9. \log_{10}/\log_{10} scatterplot of mean maximal approach velocities against standard length for ten largemouth bass, showing that approach velocities increase in direct proportion to increase in body size.

mechanism and perhaps to disproportionate changes in the resistive forces affecting the feeding mechanism.

Apparently, the shortening velocity per sarcomere of the muscles driving the feeding apparatus slowed as body size increased, which is in contrast to the assumption of our model of a constant rate of sarcomere shortening and overall muscle contraction velocity with increasing body size. The expectation from our model of unloaded muscle contraction is apparently unrealistic and the difference between our observed and expected results is probably due to the discrepancy in the scaling of muscle contraction velocity per sarcomere.

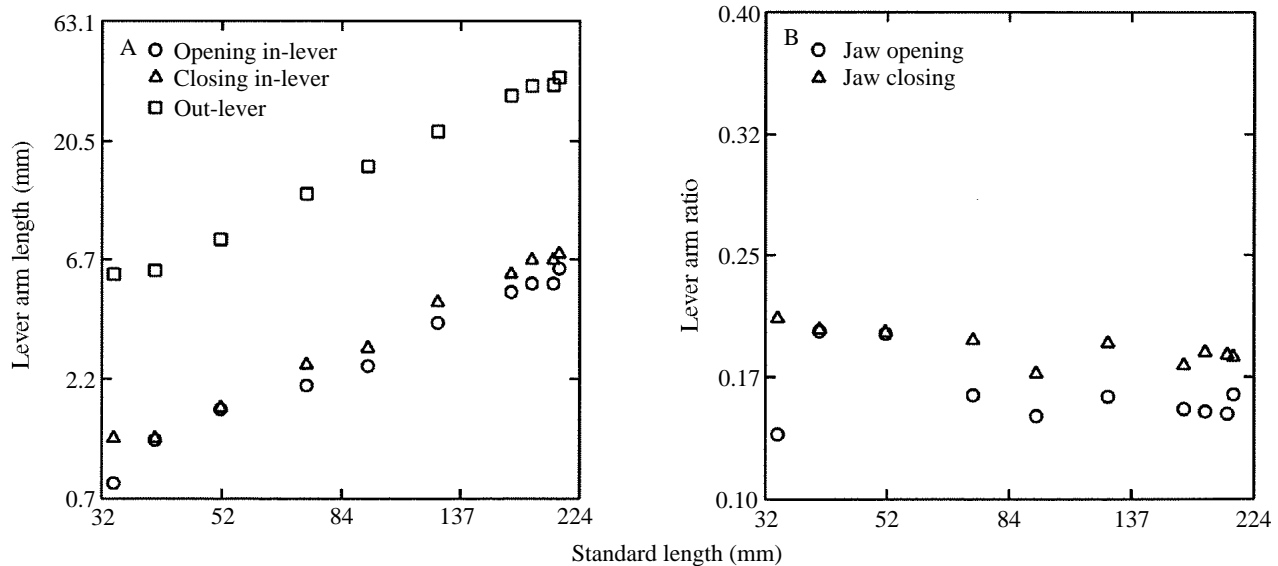


Fig. 10. \log_{10}/\log_{10} scatterplot of lower jaw lever arm lengths of the ten largemouth bass against standard length, showing that the lever arms scale isometrically (A), and a scatterplot of the lever arm ratios of opening and closing of the ten bass, plotted against standard length, showing that the ratios remain constant with increasing body size (B).

The alternative model of Hill (1950) and O'Reilly *et al.* (1993) assumes that, as body size increases, force production of the muscles powering movements increases at a slower rate than the mass of the components being moved (force scales as $\text{mass}^{2/3}$). Thus, the predictions that angular velocities would be inversely proportional to body length with a slope of -1 and the timing of feeding mechanism movements would be directly proportional to body length with a slope of 1 were even farther from the observed results than those of our model utilizing unloaded contraction velocity. All of the observed kinematic timing and velocity variable scaling relationships were significantly different from those of the alternative model, whereas nine of the 18 variables differed significantly from our model (Table 1). This is an interesting result, given that the model of Hill (1950) and O'Reilly *et al.* (1993) might be expected to be closer to reality because it incorporates the changing relative force production of muscle with increasing body size, which was not included in our model.

If we correct our model using available empirical data on the scaling of muscle contraction rates of lower vertebrates, our observed results are much closer to that predicted by our model. Data are available for the scaling of time-to-peak twitch and maximum velocity of muscle shortening for a fish (Archer *et al.* 1990), a salamander (Bennett *et al.* 1989) and a lizard (Marsh, 1988). In a study of scaling effects on muscle contractile properties of the cod *Gadus morhua* (Archer *et al.* 1990), twitch contraction time scaled with fish length with a slope of 0.29, indicating a relative slowing of muscle shortening rate with increasing size. A study of the effect of body size on muscle mechanics and locomotor performance in the salamander *Ambystoma tigrinum* (Bennett *et al.* 1989) found that time-to-peak tension in an isometric twitch scaled with body mass with a slope of 0.155 and estimated that maximal contractile velocity scaled with body mass with a

slope of -0.109 . If the preceding slopes are transformed from the scaling of mass to the scaling of length (assuming length scales to mass with a slope of 0.33), the resultant slopes are 0.465 for time-to-peak twitch and -0.327 for maximum velocity. Thus, their results also indicate a slowing of muscle contraction speed with increasing size. In a study of the scaling of muscle contractile properties and sprint performance in the lizard *Dipsosaurus dorsalis* (Marsh, 1988), a slowing of muscle contractile speed with increasing size was also found. Time-to-peak twitch scaled with a slope of 0.194 and maximal shortening velocity scaled with a slope of -0.084 , and the mass to length transformations of those slopes would yield a slope of 0.582 for time-to-peak twitch and a slope of -0.252 for maximal shortening velocity. Overall means of the above values give a slope of 0.446 for time-to-peak twitch and a slope of -0.289 for maximal unloaded contraction velocity. The slope of 0.446 for the timing of twitch contraction, when incorporated into our model as an expected scaling relationship for muscular contraction, is an indicator of change in input velocity with increasing size and would yield results that fall in the range of our observed results for timing variables, which had slopes between 0.213 and 0.584, with a mean of 0.343. The maximal unloaded contraction velocity slope of -0.289 , when incorporated into our model, would correctly predict our observed angular velocities of displacements, which had slopes ranging from -0.148 to -0.502 , with a mean of -0.305 . Our model assumed an isometric increase in the speed of muscle shortening, but it appears that, when we incorporate empirical values of muscle contractile properties into our model, the observed and predicted results are in closer accord.

One factor not considered in either model that may have important consequences for the size-dependence of muscle

performance in the largemouth bass feeding system is the scaling of forces that resist movements of the feeding apparatus through the water. Because water is 700 times more dense than air, it presents a different set of challenges to an animal attempting to accelerate body parts through the environment. Three of the four major hydrodynamic forces (pressure drag, lift and acceleration reaction) are directly proportional to the density of the medium (Denny, 1993). Our preliminary observations suggest that pressure drag and acceleration reaction, considered to be insignificant in air, are prominent in the largemouth bass feeding system. These forces would be expected to scale quite differently with body size. Drag scales as a function of the cross-sectional area of the structure being moved or as the square of linear dimensions, but the acceleration reaction is proportional to the volume of the structure or to the cube of linear dimensions. The presence of an acceleration reaction in the bass feeding system is indicated by our observation that the jaws of the fish in our study were accelerated and decelerated during prey capture (Fig. 4). The various forces that resist movement of the jaw through the water will sum but, because of the cubic power relationship of the acceleration reaction, this force should determine the exponential scaling of overall resistive forces. Interestingly, this line of reasoning suggests that the resistive forces opposing feeding apparatus movements in water may not scale more steeply than a cubic function of length. In turn, the major force resisting the acceleration of body parts in air is the mass of the moving object (Hill, 1950; O'Reilly *et al.* 1993), which also scales to length cubed. Hence, these preliminary observations suggest that, although the forces resisting acceleration of body parts in water will be higher in magnitude than the forces in air, the exponential scaling relationship may be the same in both media. An important goal in future research on the causal basis of kinematic scaling in aquatic systems will be to test this expectation by more fully modeling and measuring the forces resisting skeletal movement.

Interestingly, other scaling studies of feeding kinematics have found results rather different from those reported here. In a study of feeding kinematics of the toad *Bufo alvarius* (O'Reilly *et al.* 1993), it was found that over a large size range general body shape was maintained and that the timing of movements was proportional to linear dimensions (a proportional slowing of movements with increasing size), providing a close fit to the models proposed by Hill (1950) and O'Reilly *et al.* (1993). In a study of the scaling of feeding kinematics of the salamander *Salamandra salamandra* (Reilly, 1993), yet a third pattern was found, in which no differences in kinematic variables with increasing body size were observed in an ontogenetic series. These studies produced results markedly different from those reported here. The study of toads revealed a much greater slowing of feeding movements than was shown in our study of largemouth bass, while the salamander study found no effect of body size. Our results fall between those of these two studies. The apparent diversity of results from both feeding and locomotor studies of the scaling of kinematics suggests that some caution is warranted

regarding the degree to which the fit between our kinematic data and the adjusted model can be viewed as a causal relationship.

Comparisons with locomotor systems

In the absence of additional comparative studies of the scaling of feeding kinematics in lower vertebrates, the results of our study can be compared with those of two studies of the effect of body size on locomotor abilities. The effect of body size on sprint performance in the lizard *Dipsosaurus dorsalis* (Marsh, 1988) and the scaling of locomotor performance in the salamander *Ambystoma tigrinum* (Bennett *et al.* 1989) have been examined. When relating our results on the scaling of gape cycle time to limb cycle time of the locomotor studies, comparisons can be drawn. The above studies did not directly report the scaling of limb cycle time, but rather they reported the scaling of stride frequency (strides^{-1}), the inverse of limb cycle time. To facilitate comparisons with our results for the scaling of gape cycle time, we converted the scaling relationships for stride frequency to slopes representing limb cycle time. The inverse of stride frequency, stride time, scaled against body mass yields a slope of 0.238, indicating that limb cycle time increases with increasing body mass (Marsh, 1988). If we convert the limb cycle time slope of 0.238 to linear dimensions, the slope of limb cycle time against body length would be 0.714, which is higher than our slope of 0.430 for gape cycle time. It should be noted that both results indicate a distinct slowing of movements with increasing body size. The results of the scaling study of salamander locomotor performance (Bennett *et al.* 1989) contrast with those for lizards (Marsh, 1988) and with those of the present study, in that no effect of body size on leg cycling frequency was found, although this effect was found for feeding kinematics in the salamander *S. salamandra* (Reilly, 1993). The regression of leg cycling frequency against body mass had a slope of 0.080, indicating that limb cycle frequency, and therefore limb cycle time, did not change significantly with increasing body size. Given the diversity of results that have been observed for the scaling of feeding and locomotor kinematics in lower vertebrates, it is not possible to delineate any general patterns at this time. Thus, it appears that more work on the scaling of both feeding and locomotor kinematics will be needed before any general patterns of the effects of body size on movements can be proposed.

Implications for comparative studies

The results of this study strongly indicate the need to account for body size in future comparative studies of feeding kinematics. Our finding that body size had major effects on kinematic timing and velocity variables suggests that comparing feeding kinematics of animals of different body size should only be performed when body size effects are taken into account. For example, if one were to compare prey capture kinematics between two species of fish, one of large body size and the other of small body size, one might expect that the larger fish species would have slower movements of the

feeding apparatus based on body size difference alone and not necessarily because of any differences in functional ability of the feeding mechanisms. We note that most previous comparative feeding studies have attempted to account for body size effects by limiting the size range of individuals of the species under consideration (Shaffer and Lauder, 1985; Larsen *et al.* 1989; Reilly and Lauder, 1992). In addition, the relevant variable of concern with regard to body size may be some direct measure of the feeding mechanism, such as jaw length or mouth gape, rather than an overall measure of body size, such as standard length or body mass.

Further caution is suggested because our results indicate that the effects of body size on kinematics can be complex. For example, consider our results for the analysis of the shape of the gape cycle profile (Fig. 7B). With increasing body size, there is a change in the proportion of the gape cycle made up by opening and closing movements. Thus, gape cycles of differently sized taxa may not be directly comparable in size (duration) or shape. Body size effects on kinematics may be lessened in comparative studies by choosing specimens of similar size or by using analysis of covariance, with body size as the covariate in instances where a similar range of body sizes is used for each taxon. Additional studies will be needed to assess fully the significance of scaling relationships on feeding kinematics and its impact on comparative studies. The comparative data of our study taken with those of O'Reilly *et al.* (1993) and Reilly (1993) suggest that there is no general pattern for the scaling of feeding kinematics. Thus, because of the unpredictable nature of the effect of body size on feeding kinematics, it will be advisable for future studies to gather empirical data for the taxa under investigation.

Kinematics and feeding ecology

The ontogeny of diet of largemouth bass typically involves at least one major diet shift that usually occurs in the size range 80–100mm SL (Keast, 1985; Werner, 1977). The abrupt shift is from a diet dominated by benthic invertebrates to one consisting almost exclusively of other fishes. One interesting result of this study is that we found no distinct shifts in functional ability in our size series of largemouth bass, which encompassed the size range of the typical diet shift of largemouth bass. All kinematic variables changed in a continuous fashion with increasing body size. Thus, we find no evidence to support the notion that the diet shifts of largemouth bass are driven by dramatic shifts in functional ability occurring at the body sizes where diet shifts usually occur.

We thank T. Bevis for giving us access to his property to collect the specimens used in this study. Thanks go to T. Bevis and S. Richard for help in collecting specimens. We greatly appreciate the continual supply of prey-fish for this study provided by C. Johnson. T. Moerland, K. Rebello, J. Travis and R. Turingan offered valuable comments throughout the study and on the manuscript. We thank J. O'Reilly, S. Reilly and M. LaBarbera, who shared with us their unpublished data

and thoughts on the scaling of musculo-skeletal systems. This research was supported by a Florida State University CRC-Planning grant and NSF grant IBN-9306672 to P.C.W.

References

- ALEXANDER, R. MCN. (1969). Mechanics of the feeding action of a cyprinid fish. *J. Zool., Lond.* **159**, 1–15.
- ARCHER, S. D., ALTRINGHAM, J. D. AND JOHNSTON, I. A. (1990). Scaling effects on the neuromuscular system, twitch kinetics and morphometrics of the cod, *Gadus morhua*. *Mar. Behav. Physiol.* **7**, 137–146.
- BAREL, C. D. N. (1983). Towards a constructional morphology of the cichlid fishes (Teleostei, Perciformes). *Neth. J. Zool.* **33**, 357–424.
- BENNETT, A. F., GARLAND, T., JR AND ELSE, P. L. (1989). Individual correlation of morphology, muscle mechanics and locomotion in a salamander. *Am. J. Physiol.* **256**, R1200–R1208.
- CALDER III, W. A. (1984). *Size, Function and Life History*. Cambridge, MA: Harvard Press.
- DENNY, M. W. (1993). *Air and Water: the Biology and Physics of Life's Media*. Princeton, NJ: Princeton University Press.
- GANS, C. AND GORNIK, G. C. (1982). How does the toad flip its tongue? *Science* **216**, 1335–1337.
- GARLAND, T., JR (1985). Ontogenetic and individual variation in size, shape and speed, in the Australian agamid lizard *Amphibolurus nuchalis*. *J. Zool., Lond.* **207**, 425–439.
- HIEMAE, K. M. AND CROMPTON, A. W. (1985). Mastication, food transport and swallowing. In *Functional Vertebrate Morphology* (ed. M. Hildebrand, D. M. Bramble, K. F. Liem and D. B. Wake), pp. 262–290. Cambridge: Cambridge University Press.
- HIEMAE, K. M., THEXTON, A., MCGARRICK, J. AND CROMPTON, A. W. (1981). The movement of the cat hyoid during feeding. *Arch. oral Biol.* **26**, 65–81.
- HILL, A. V. (1950). The dimensions of animals and their muscular dynamics. *Sci. Prog., Lond.* **38**, 209–230.
- KATZ, S. L. AND GOSLINE, J. M. (1993). Ontogenetic scaling of jump performance in the African desert locust (*Schistocerca gregaria*). *J. exp. Biol.* **177**, 81–111.
- KEAST, A. (1985). The piscivore feeding guild of fishes in small freshwater ecosystems. *Env. Biol. Fish.* **12**, 119–129.
- LARSEN, J. H., JR AND BENESKI, J. T., JR (1988). Quantitative analysis of feeding kinematics in dusky salamanders (*Desmognathus*). *Can. J. Zool.* **66**, 1309–1317.
- LARSEN, J. H., JR, BENESKI, J. T. AND WAKE, D. B., JR (1989). Hyolingual feeding systems of the Plethodontidae: comparative kinematics of prey capture by salamanders with free and attached tongues. *J. exp. Zool.* **252**, 25–33.
- LAUDER, G. V. (1983). Food capture. In *Fish Biomechanics* (ed. P. W. Webb and D. Weihs), pp. 280–311. New York: Praeger Publishers.
- LAUDER, G. V. (1985). Aquatic feeding in lower vertebrates. In *Functional Vertebrate Morphology* (ed. M. Hildebrand, D. M. Bramble, K. F. Liem and D. B. Wake), pp. 210–229. Cambridge: Cambridge University Press.
- LIEM, K. F. (1978). Modulatory multiplicity in the functional repertoire of the feeding mechanism in cichlid fishes. *J. Morph.* **158**, 323–360.
- MARSH, R. L. (1988). Ontogenesis of contractile properties of skeletal muscle and sprint performance in the lizard *Dipsosaurus dorsalis*. *J. exp. Biol.* **137**, 119–139.
- MILLER, B. T. AND LARSEN, J. H., JR (1990). Comparative kinematics

- of terrestrial prey capture in salamanders and newts (Amphibia: Urodela: Salamandridae). *J. exp. Zool.* **256**, 135–153.
- NISHIKAWA, K. AND CANNATELLA, D. (1991). Kinematics of prey capture in the tailed frog *Ascaphus truei* (Anura: Ascaphidae). *Zool. J. Linn. Soc.* **103**, 289–307.
- NYBERG, D. W. (1971). Prey capture in the largemouth bass. *Am. Midl. Nat.* **86**, 128–144.
- O'REILLY, J. C., LINDSTEDT, S. L. AND NISHIKAWA, K. C. (1993). The scaling of feeding kinematics in toads (Anura: Bufonidae). *Am. Zool.* **33**, 147A.
- REILLY, S. M. (1993). The ontogeny of feeding kinematics in salamanders: is aquatic feeding behavior innate or influenced by learning? *Am. Zool.* **33**, 147A.
- REILLY, S. M. AND LAUDER, G. V. (1992). Morphology, behavior and evolution: comparative kinematics of aquatic feeding in salamanders. *Brain Behav. Evol.* **40**, 182–196.
- RICKER, W. E. (1973). Linear regressions in fishery research. *J. Fish. Res. Bd Can.* **30**, 409–434.
- SCHMIDT-NIELSEN, K. (1984). *Scaling: Why is Animal Size so Important?* Cambridge: Cambridge University Press.
- SCHWENK, K. AND THROCKMORTON, G. S. (1989). Functional and evolutionary morphology of lingual feeding in squamate reptiles: phylogenetics and kinematics. *J. Zool., Lond.* **219**, 153–175.
- SCHWENK, K. AND WAKE, D. B. (1993). Prey processing in *Leurognathus marmoratus* and the evolution of form and function in desmognathine salamanders (Plethodontidae). *Biol. J. Linn. Soc.* **49**, 141–162.
- SHAFFER, H. B. AND LAUDER, G. V. (1985). Patterns of variation in aquatic ambystomatid salamanders: kinematics of the feeding mechanism. *Evolution* **39**, 83–92.
- SHAFFER, H. B. AND LAUDER, G. V. (1988). The ontogeny of functional design: metamorphosis of feeding behavior in the tiger salamander (*Ambystoma tigrinum*). *J. Zool., Lond.* **216**, 437–454.
- SMITH, K. K. (1982). An electromyographic study of the function of the jaw adducting muscles in *Varanus exanthematicus* (Varanidae). *J. Morph.* **173**, 137–158.
- SMITH, K. K. (1984). The use of the tongue and hyoid apparatus during feeding in lizards (*Ctenosaura similis* and *Tupinambis nigropunctatus*). *J. Zool., Lond.* **202**, 115–143.
- THEXTON, A. J. AND CROMPTON, A. W. (1989). Effect of sensory input from the tongue on jaw movement in normal feeding in the opossum. *J. exp. Zool.* **250**, 233–243.
- UPDEGRAFF, G. (1990). *Measurement TV: Video Analysis Software*. San Clemente, CA: Data Crunch.
- WAINWRIGHT, P. C. AND RICHARD, B. A. (1995). Predicting patterns of prey use from morphology in fishes. *Env. Biol. Fish.* (in press).
- WERNER, E. E. (1974). The fish size, prey size, handling time relation in several sunfishes and some implications. *J. Fish. Res. Bd Can.* **31**, 1531–1536.
- WERNER, E. E. (1977). Species packing and niche complementarity in three sunfishes. *Am. Natr.* **111**, 553–578.
- WESTNEAT, M. W. (1990). Feeding mechanics of teleost fishes (Labridae; Perciformes): a test of four-bar linkage models. *J. Morph.* **205**, 269–295.
- WILKINSON, L. (1992). *SYSTAT for Windows, Version 5*. Evanston, IL: SYSTAT, Inc.
- ZWEERS, G. A. (1974). Structure, movement and myography of the feeding apparatus of the mallard (*Anas platyrhynchos L.*): a study in functional anatomy. *Neth. J. Zool.* **24**, 323–467.